



Acycle: Time-series analysis software for paleoclimate research and education



Mingsong Li^{a,*}, Linda Hinnov^b, Lee Kump^a

^a Department of Geosciences, The Pennsylvania State University, University Park, PA, 16802, USA

^b Department of Atmospheric, Oceanic, and Earth Sciences, George Mason University, Fairfax, VA, 22030, USA

ARTICLE INFO

Keywords:

Data processing
Geology
Cyclostratigraphy
Stratigraphy
Sedimentology
Algorithms

ABSTRACT

Recognition and interpretation of paleoclimate signals in sedimentary proxy datasets are time consuming and subjective. *Acycle* is a comprehensive and easy-to-use software package for time series analysis in paleoclimate research and education. It is designed to speed paleoclimate time series analysis, especially cyclostratigraphy, and to provide objective methods for estimating astrochronology. *Acycle* provides for detrending with multiple options to track and remove secular trends. A selection of power spectral analysis methodologies is offered for the detection of periodic signals. Many of the functions are specific to cyclostratigraphy and astrochronology that are not found in standard statistical packages. A specialized function is provided to assess the astronomical (Milankovitch) forcing of paleoclimate series and search for the most likely sedimentation rate by evaluating the correlation coefficient between power spectra of an astronomical solution and sedimentary proxy data. Sedimentary noise modeling (for past sea-level changes) is also provided in *Acycle*. As an example, *Acycle* is applied to a sedimentary proxy series from the cyclostratigraphy of the Paleocene-Eocene thermal maximum (PETM) in Core BH9/05 from the Paleogene Central Basin, Svalbard. *Acycle* detects significant astronomical forcing in the proxy series and relatively stable sedimentation rates during and after the PETM. *Acycle* runs in the MATLAB environment or as stand-alone software on Windows and Macintosh OS X, and is open-source software.

1. Introduction

Time series analysis plays a fundamental role in the natural sciences. In growing important geoscience application, recognition and interpretation of (quasi-) periodic astronomical (Milankovitch) signals in sedimentary records can be time consuming and subjective. Many analysis steps are required in time series analysis, including detrending (to remove long-term secular trends), power spectral analysis (to evaluate periodicity in signals), evolutionary power spectral analysis (for tracking time-variable periodicity in signals), and hypothesis tests (for assessing signal-to-noise ratios) (Ghil, 1997; Kodama and Hinnov, 2015; Mann and Lees, 1996; Thomson, 2009; Weedon, 2003). Methods of evaluating sediment accumulation rates include the average spectral misfit (ASM) (Meyers and Sageman, 2007), Bayesian Monte Carlo (Malinverno et al., 2010), TimeOpt (Meyers, 2015), evolutive TimeOpt (Meyers, 2019), and correlation coefficient (COCO) (Li et al., 2018c) approaches. The selection of parameters for these (and other procedures in *Acycle*) can be complex and have a significant influence on the interpretation.

Three reasons motivated the development of the *Acycle* time series

analysis program: (1) There is a need to broaden and encourage the experience of time series analysis in the geosciences, especially in cyclostratigraphy. (2) There is a need to speed the process for the time-series analysis steps (detailed in Section 4), which can be very time-consuming. (3) There is a need to provide objective methods for the analysis of paleoclimate signals as reproducibility becomes a major challenge.

The *Acycle* software package integrates the analysis of paleoclimate time series using the MATLAB programming language. The functions accommodate independent variables of any dimension, but typically, paleoclimate data present first in the stratigraphic (depth) domain with units in cm, m, etc., and once a sedimentation rate is applied to the data (or the data are otherwise tuned), in the time domain with units in years, kyr, etc. *Acycle* also runs as a stand-alone program on Windows and Macintosh OS platform with multiple language versions. The software is powerful, but easy-to-use with its graphical user interface (GUI). *Acycle* should benefit research and education in the closely allied fields of paleoclimatology, paleoceanography, cyclostratigraphy, and astrochronology.

In this paper, we introduce the structure of *Acycle*, accepted styles of

* Corresponding author. 410 Deike Bldg, University Park, PA, 16802, USA.

E-mail addresses: mul450@psu.edu, limingsonglms@gmail.com (M. Li), lhinno@gmu.edu (L. Hinnov), lrk4@psu.edu (L. Kump).

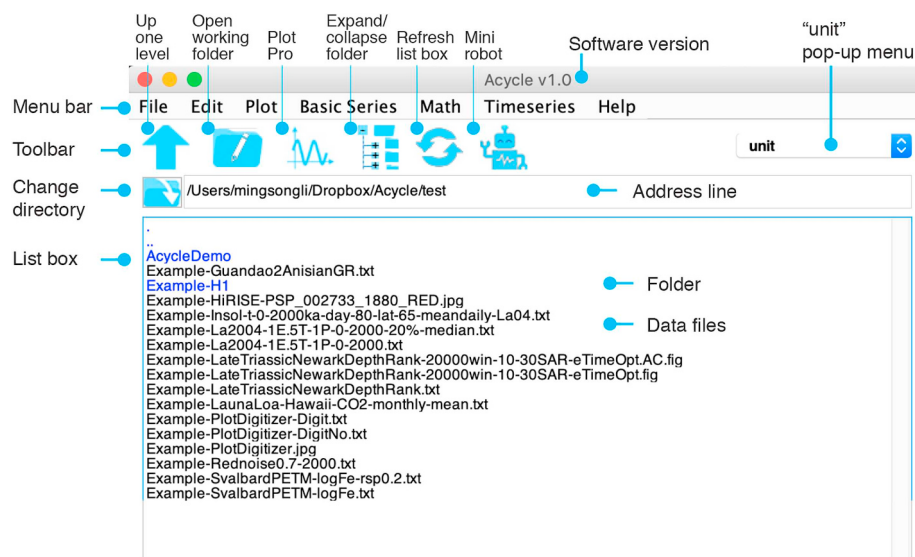


Fig. 1. *Acycle* graphical user interface (GUI).

data inputs and outputs, and the functions provided for the time series analysis of paleoclimate signals. There is an emphasis on methods and toolboxes that are not available in other similar software packages. Similarities and differences between *Acycle* and other similar applications (e.g., *AnalySeries* (Paillard et al., 1996), *Astrochron* (Meyers, 2014), *REDFIT* (Schulz and Mudelsee, 2002), and *PAST* (Hammer et al., 2001), among others) are discussed briefly. Functionality is demonstrated with an analysis of a paleoclimate data series from the Paleocene-Eocene Thermal Maximum interval that is included in *Acycle* as a test case.

2. *Acycle* software structure

The software includes a menu bar, a toolbar, an address line, and a list box (Fig. 1). The menu bar provides access to functions and various toolboxes (Fig. 2), e.g., functions for file editing and plotting, access to demonstration time series, time series toolboxes, and Help documents. The toolbar enables quick access to frequently used functions and toolboxes, e.g., clicking on the “Refresh” button triggers the program to refresh the list box and “Unit” for the unit selection. The list box displays files and folders within the directory in the address line.

3. Data inputs and outputs

The input file containing a paleoclimate series can be in a variety of formats, including table- or space-delimited text, or comma-separated values files from an Excel-type spreadsheet. The data file must contain two columns with values. The first column must be depth or time, and the second column must contain the values that are assigned to the corresponding depth or time. All data files, plots, and folders are displayed in the GUI list box (Fig. 1). A couple of example data files can be accessed at “Examples” under the “Basic series” menu (Fig. 2).

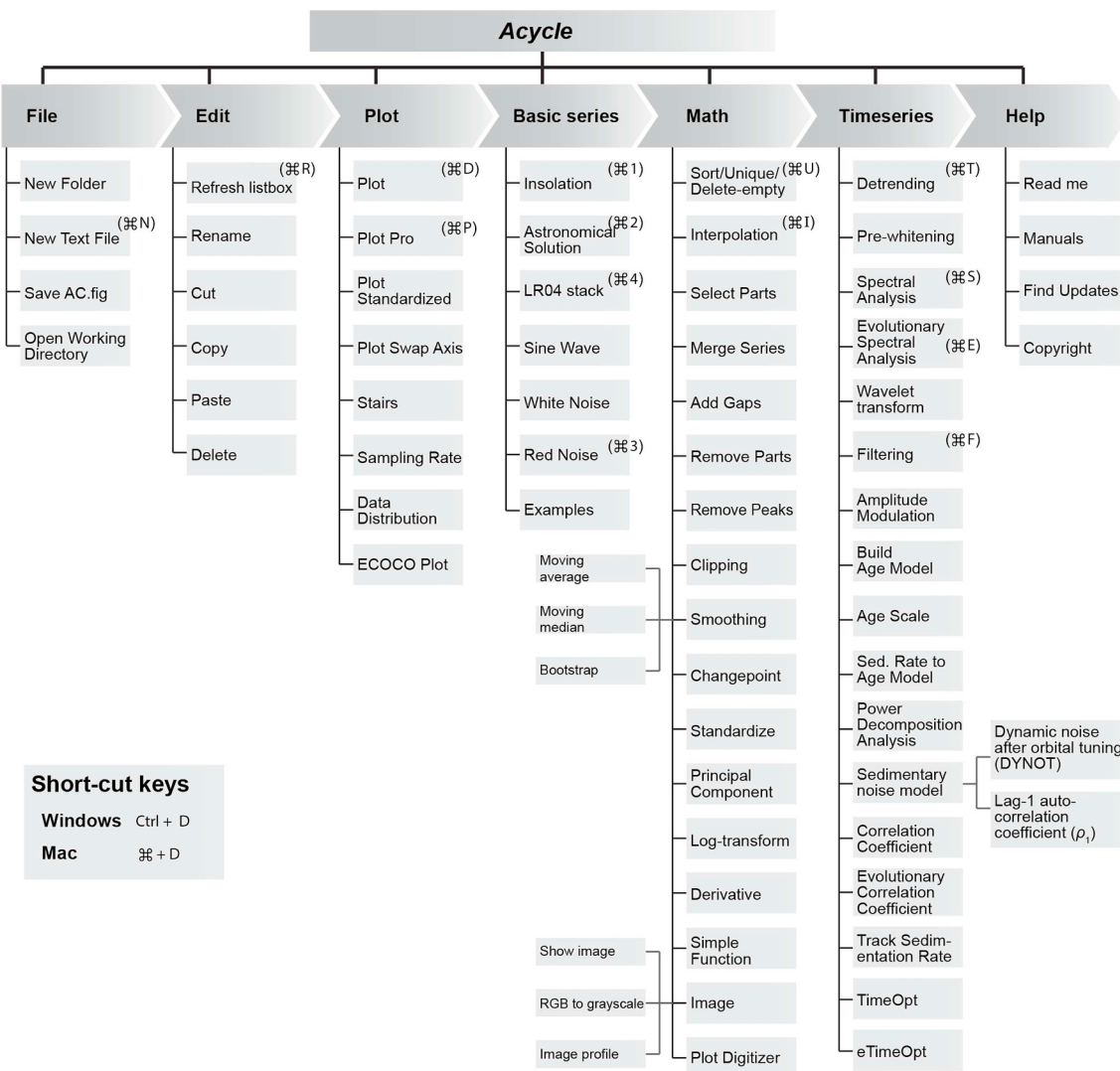
The user can output data series in *.txt or *.csv type using the appropriate menu. Generally, *Acycle* will show all generated figures (plots), and the user will ultimately decide which ones should be saved. The plots can be saved as raster images, vector images, or MATLAB Figure (*.fig) file. Supported output raster image types include JPEG (*.jpg), Bitmap (*.bmp), Portable Network Graphics (*.png), and TIFF (*.tif). Vector images include Portable Document Format (.pdf) and Scalable Vector Graphics (*.svg).

4. Typical procedures in cyclostratigraphy

The identification of potential astronomical signals in stratigraphic data series using *Acycle* involves the following steps:

- (1) Users must formulate the data in an input format accepted by *Acycle* (Section 3).
- (2) Original data may need sorting, removing empty values, or averaging multiple values assigned to the same depth (time) (Section 4.2).
- (3) The data must be interpolated to a uniform sampling interval (Section 4.3).
- (4) Detrending is usually useful (Section 4.4).
- (5) Power spectral analysis is used to identify dominant frequencies (Section 4.5). Fitting a red noise model to the background spectrum can help to determine which spectral peaks are significantly different from noise.
- (6) Users may need evolutionary power spectral analysis for inspecting changes in frequency patterns through the data series (Section 4.6).
- (7) A method that applies a correlation coefficient approach jointly determines optimal sedimentation rate and tests the null hypothesis that no Milankovitch frequency is present in the data (Section 4.7).
- (8) Based on the wavelengths (stratigraphic thicknesses) of prominent cycles in a stratigraphic data series, and an assumed sedimentation rate, filtering tools may be applied to isolate specific frequency bands (Section 4.8).
- (9) Stratigraphic data series may be correlated/tuned using the “Age Scale” function in *Acycle* based on the astronomical cycles inferred from filtering (Section 4.9).
- (10) Other approaches are provided to decipher hidden information in the data, for example, a sedimentary noise model for stratigraphic data from marginal marine successions that are linked to sea level changes (Section 4.10).

Steps 3–10 are commonly time-consuming, and Steps 2–6 can be done automatically with a “mini-robot” imbedded in *Acycle* (Fig. 1). Below *Acycle* capabilities are demonstrated using a paleoclimate series described in Section 4.1, with emphasis on key steps and new approaches that are not provided in other software (e.g., sedimentation rate evaluation by correlation coefficient, COCO and eCOCO, and sedimentary noise modeling, DYNOT).

**Fig. 2.** Acycle components.

4.1. The demonstration paleoclimate series

The paleoclimate series used to demonstrate *Acycle* is the XRF-generated iron (Fe) concentration series of Core BH9/05 from the Paleogene Central Basin of Spitsbergen, Svalbard (Fig. 3). The full Fe series of the Paleocene-Eocene Frysjaodden Formation was studied by Charles et al. (2011) to construct an astrochronology for the global carbon cycle perturbation associated with the Paleocene-Eocene thermal maximum (PETM) (Gui et al., 2011). The Central Basin of Spitsbergen developed as a foreland basin receiving muddy sediments during Paleocene-Eocene time (Charles et al., 2011). The lithology at Core BH9/05 is dominated by mudstone and black shales. Fe is a proxy of terrestrial input into the Central Basin.

4.2. Data preparation

Acycle includes several toolboxes to facilitate data preparation. Users can sort data in ascending or descending order. Two or more values for the same time (or depth) may be averaged with the “Unique” function. A portion of the data series can be read or saved with user-defined values, in time (or depth, the first column) and value (the second column). Other useful tools include a moving average function and a first-difference function (Fig. 2).

Many established statistical tests assume that the evaluated data

have a Gaussian (normal) distribution (Weedon, 2003). However, natural processes may have “non-Gaussian” distribution, which can lead to difficulties of an evaluation (Kodama and Hinnov, 2015). The climate response of a sedimentary proxy to forcing may be non-linear (Herbert, 1994; Martinez, 2018), or the variance of the series can be very large (Charles et al., 2011), or the distribution might be asymmetric (Prokopenko et al., 2006). Log-transformation, which is included in *Acycle*, is frequently used to convert a time series that has a skewed distribution to one that spans a much smaller range and is closer to “Gaussian” (Kodama and Hinnov, 2015); this is true for the demonstration paleoclimate series here. Log-transformation can be applied only to strictly positive values; negative numbers can be handled by adding a positive constant so that all values become positive (Weedon, 2003).

4.3. Sampling rate and interpolation

Acycle includes functions to assess the sampling rate of the time series. Stratigraphic depth or time series are typically irregularly spaced due to uncertain timescales or difficulty in data collection (Martinez et al., 2016). This necessitates interpolation to generate uniformly spaced time (or depth) series. While several applications, such as SPECTRUM (Schulz and Stattegger, 1997) and REDFIT (Schulz and Mudelsee, 2002) apply the Lomb-Scargle periodogram for non-

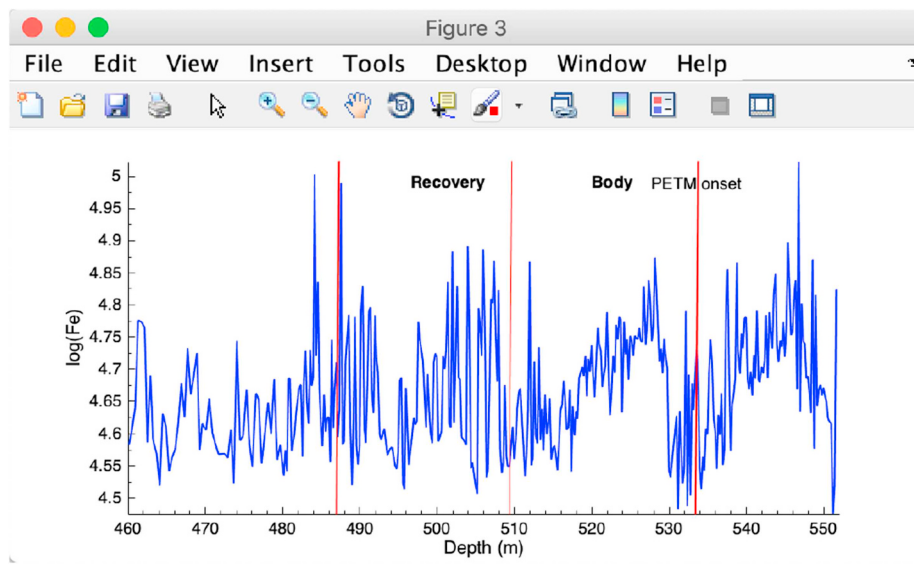


Fig. 3. Log-transformed Fe paleoclimate series from 552 m to 460 m at Core BH9/05 in the Paleocene Central Basin of Svalbard. The Fe series is shown with PETM event onset and “body” interval of a prominent negative carbon isotope excursion, followed by gradual recovery stages (Cui et al., 2011). These data are from Charles et al. (2011): <https://agupubs.onlinelibrary.wiley.com/action/downloadSupplement?doi=10.1029/2F2010GC003426&file=ggge1904-sup-0002-ts01.xls>.

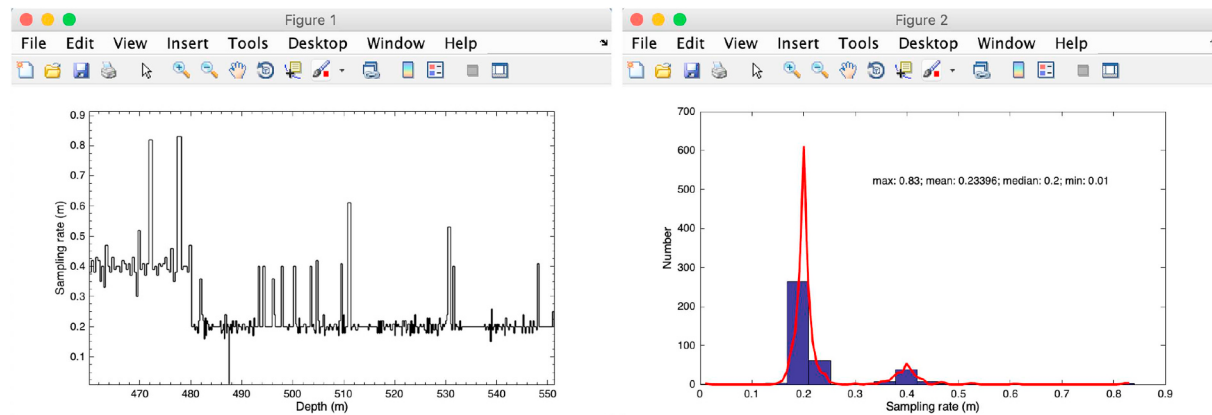


Fig. 4. Left panel: Sample rate of the Log(Fe) series of Core BH9/05 from the Paleogene Central Basin of Svalbard. Right panel: Histogram and the “kernel” fit of the sample rates. Two peaks are centered at 0.2 and 0.4, respectively. These plots were generated using the “Sampling Rate” function in the “Plot” menu (Fig. 2).

uniformly spaced time series, other powerful techniques such as multitaper spectral analysis require uniformly sampled time series.

The user should be careful when interpolating irregularly spaced data to a uniform sampling rate. If hypothesis testing is to be performed with null models based on autoregressive noise, then the selected sample rate (Δt) is crucial (detailed below and Eq. (4)) (Martinez et al., 2016). Weodon (2003) recommends a minimum of four points per major oscillation despite the strict definition of the Nyquist frequency ($f_N = 1/(2^* \Delta t)$) of two samples per cycle. Prokopenko et al. (2006) concluded that interpolating to a rate close to the average sampling rate of an irregularly spaced stratigraphic dataset could result in loss of information of high-frequency signals. When interpolation is needed, one option is to interpolate the data using a sample interval that is half that of the thinnest visible bed (Weodon, 2003).

The sample rate-dependent power spectrum of the first order autoregressive (AR(1)) process is for frequency f (e.g., Mann and Lees, 1996):

$$S(f) = S_0 \frac{1 - \rho_1^2}{1 - 2\rho_1 \cos\pi\left(\frac{f}{f_N}\right) + \rho_1^2} \quad (1)$$

S_0 is the average value of the power spectrum, related to the white-noise variance by:

$$S_0 = \sigma^2 / (1 - \rho_1^2) \quad (2)$$

f_N , the Nyquist frequency, is the highest frequency that can be resolved for sample rate Δt , and

$$\sigma^2 = \frac{1}{n} \sum_{i=1}^n \left(x_i - \frac{1}{n} \sum_{i=1}^n x_i \right)^2 \quad (3)$$

The lag-1 autocorrelation coefficient (ρ_1) is (e.g., Mudelsee, 2002):

$$\rho_1 = \sum_{i=2}^n x_i * x_{i-1} / \sum_{i=2}^n x_{i-1}^2 \quad (4)$$

where x is the time series and n is the total number of uniformly sampled points in x . Both x and n are dependent on Δt . Therefore, over-interpolation leads to a higher ρ_1 and an incorrect estimation of conventional red noise background spectrum (Husson, 2014). Alternatively, a median or average sample distance for interpolation generates a more reasonable red-noise background.

In the demonstration paleoclimate series, the original sample rate of the log(Fe) series of Core BH9/05 is bimodal, above 480 m and below 480 m. The series as a whole has a mean sampling rate of 0.23 m and a median sampling rate of 0.2 m (Fig. 4). We interpolate the Fe series using a $\Delta t = 0.2$ m sample rate.

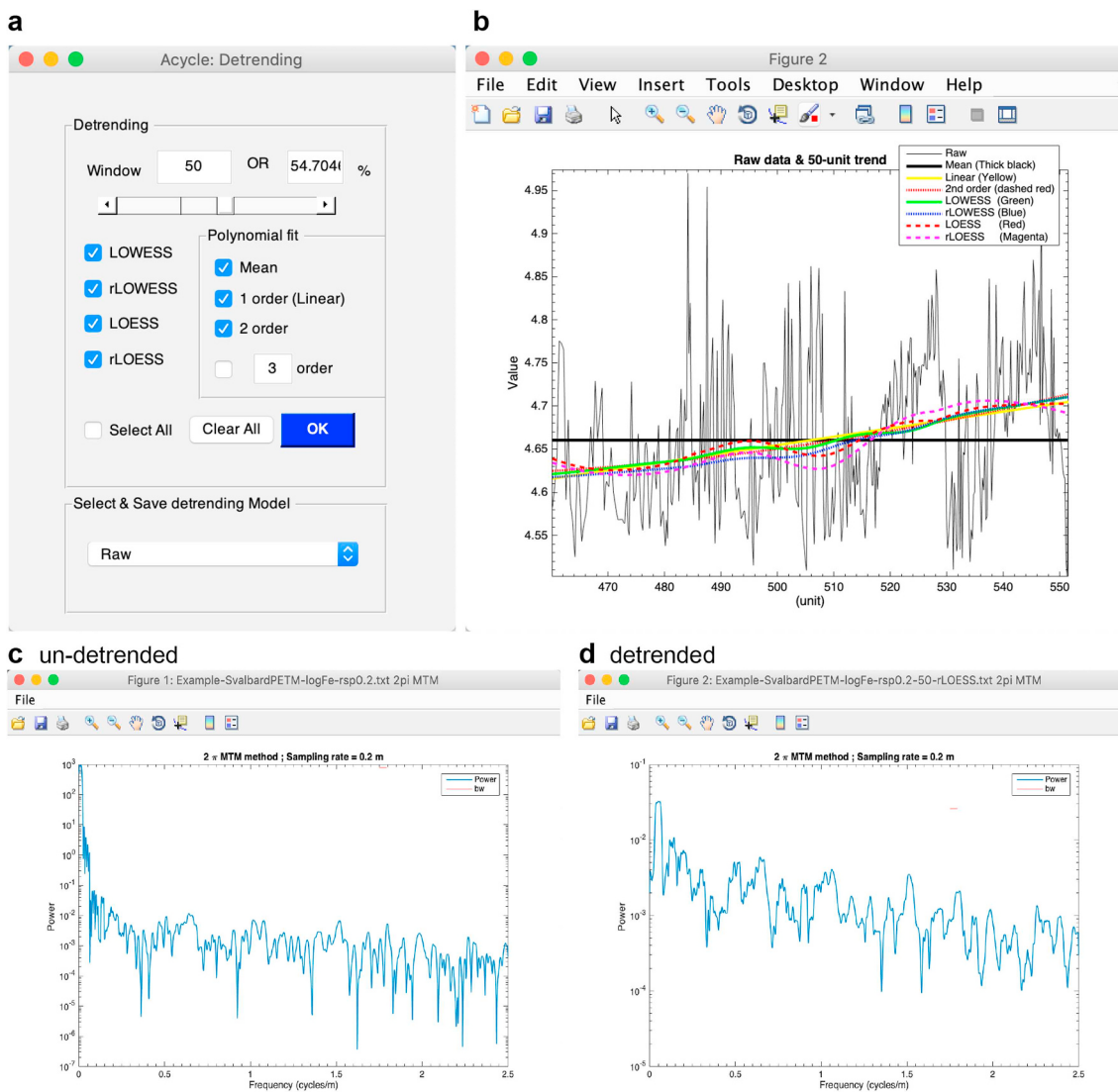


Fig. 5. (a) The “Detrending” GUI. (b) The log(Fe) series of Core BH9/05 is shown with the mean, linear trend, second order polynomial fit, and various 50-m smoothed secular trends using MatLab’s “LOWESS”, “rLOWESS”, “LOESS”, and “rLOESS” methods. (c) 2π MTM power spectrum of un-detrended data. (d) 2π MTM power spectrum of detrended data removing a 50-m “rLOESS” trend.

4.4. Detrending

Detrending is a key step in time series analysis. Time series can have secular trends that are high amplitude and irregular, causing the bulk of the data variability to be preferentially above or below the overall mean value (Rodionov, 2006). Removal of these long-term trends, or detrending, is a critical step for power spectral analysis to ensure that data variability oscillates about a zero mean, and to avoid power leakage from very low-frequency components into higher frequencies of the spectrum (Kodama and Hinnov, 2015).

Various “detrending” methods are provided in *Acycle* to estimate and remove a secular trend (Fig. 5). These include high-pass filtering (see section 4.8), polynomial fit, moving average, local regression smoothing (LOWESS and LOESS) and their robust versions (rLOWESS and rLOESS) that assign lower weight to outliers in the regression. This requires the user to identify the most appropriate smoothing window. The Mathworks Help Documentation on *smooth.m* includes a detailed description of the algorithms used for the local regression techniques.

4.5. Power spectral analysis

Power spectral analysis has become a cornerstone in paleoclimatology and cyclostratigraphy. Power spectral analysis evaluates the distribution of time series variance (power) as a function of frequency. The primary use of power spectral analysis is for the recognition of periodic or quasi-periodic components in a data series (Weedon, 2003).

The power spectrum can be evaluated with various nonparametric or parametric approaches. The frequently used nonparametric based spectral methods include the smoothed periodogram, Blackman-Tukey correlogram, and multi-taper method (MTM) estimators (Kodama and Hinnov, 2015; Weedon, 2003). Among these, the MTM estimator achieves the optimal trade-off between frequency resolution and statistical confidence for uniformly spaced time series (Thomson, 1982). For irregularly sampled time series in geosciences, the Lomb-Scargle periodogram (Lomb, 1976; Scargle, 1982) can avoid spectral distortion generated by interpolation. Basic descriptions of power spectral analysis and allied procedures are given in Box and Jenkins (1976);

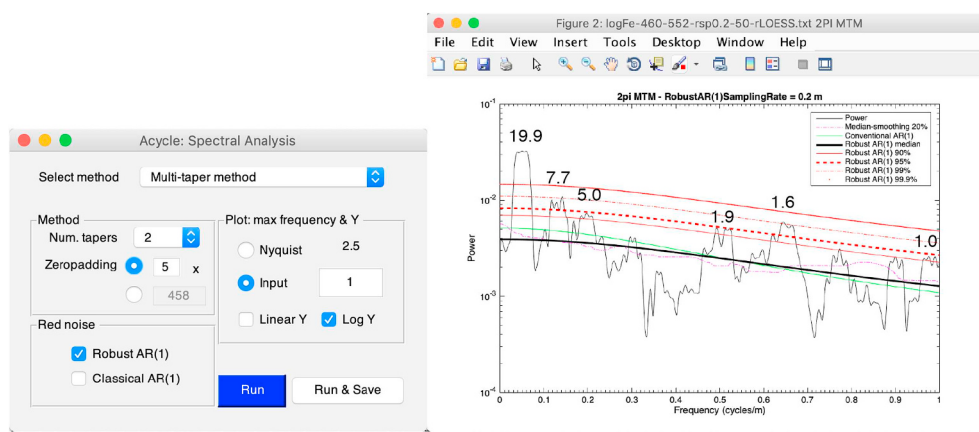


Fig. 6. Left panel: The “Spectral Analysis” GUI. Right panel: 2π multitaper (MTM) power spectrum (solid black) of the Log(Fe) series at Core BH9/05 after removing the 50 m “rLOESS” trend and interpolation of 0.2 m sample rate. The spectrum showing red-noise fit to the spectrum (solid green) based on the conventional AR(1) model. The 20% median-smoothed spectrum is also shown (dashed pink). The red-noise fit to the spectrum based on the robust AR(1) model (thick black) and 90% (solid red), 95% (dashed red), 99% (red dash-dot), 99.9% (dot) confidence limits are based on the best fit to the log power of the median-smoothed background spectrum. Cycle wavelengths are marked (in m) at top of selected spectral peaks. (For interpretation of the references to color in this figure legend, the reader is referred to the Web version of this article.)

Kodama and Hinnov (2015); Weedon (2003), and Kodama and Hinnov (2015).

The confidence level of a frequency component in a time series depends on the nature of background noise in the time series and the statistical model used to estimate the background noise. The first-order autoregressive AR(1) model (Eq. (4)) is a simple model for a discrete finite red noise series (Gilman et al., 1963; Mudelsee, 2010). The AR(1) model can be biased if the time series also contains a strong periodic or quasiperiodic signal (Hinnov et al., 2016; Mann and Lees, 1996). A time series may also have a spectrum that does not fit that of an AR(1) process, with different distributions of power at low and high frequencies. Consequently, Mann and Lees (1996) proposed a least-squares analytic fit of the AR(1) model to a median-smoothed spectrum estimate, which is known as robust AR(1) model. The goal of the model is to remove signal contributions from the series prior to the AR(1) modeling, assuming that high power “outliers” are signal contributions. These models are extensively used in paleoclimate studies. *Acycle* includes both conventional and robust AR(1) modeling options.

The 2π multitaper (MTM) power spectrum of the Log(Fe) stratigraphic series shows significant peaks above 95% confidence interval at 19.9 m, 7.7 m, 1.9 m and 1.6 m (Fig. 6) and above 90% confidence interval at 5.0 m and 1.0 m. Previous work (Charles et al., 2011) suggests that the sedimentation rate is 21.5 cm/kyr for the Svalbard data series. Therefore, the above stratigraphic cycles probably represent ~93 kyr (short orbital eccentricity), 36 kyr (obliquity), 23 kyr (precession), and three sub-Milankovitch cycles of 8.8 kyr, 7.4 kyr and 4.7 kyr. This assumption will be tested later in Section 4.7.

4.6. Evolutionary power spectral analysis

The spectral power can vary with depth or time, especially for paleoclimatic and cyclostratigraphic series, being a natural property of most geoscientific data and leading to potential distortion of paleoclimate signals in depth domain (Kodama and Hinnov, 2015; Li et al., 2018c; Weedon, 2003). When the length of the time series is longer than the cyclicity of interest, then it is possible to generate power spectra from many segments of the time series, given that each segment is long enough for detection of all cycle frequencies of interest. This is variously known as evolutionary (evolutive) spectral analysis, and sliding-window (running-window) spectral analysis (Kodama and Hinnov, 2015; Li et al., 2018b; Meyers and Hinnov, 2010; Meyers et al., 2012; Weedon, 2003).

Acycle provides options for evolutionary FFT, MTM, and Lomb-Scargle spectral analysis. User-defined parameters for these methods can be modified in the “Evolutionary Spectral Analysis” GUI, including

sliding window length and step, maximum output frequency, and 2D/3D plot options. (Fig. 7).

It is worth noting that the sliding (running) window is a key parameter of the evolutionary power spectral analysis. If the window is too long, high frequencies will be overly smoothed, possibly not detected, and if the window is too short, low frequencies will not be detected adequately (Kodama and Hinnov, 2015). As an example, because the longest cycle of interest in the log(Fe) series of Core BH9/05 is ~20 m, a slightly longer window of 25 m is adopted (Fig. 7). The evolutionary FFT shows the 20-m cycles are consistent throughout the series. The 5 m precession cycles and 1.6–1.9 m sub-Milankovitch cycles appear at the ~475–520 m interval (Fig. 7).

4.7. Evolutionary correlation coefficient

The *Acycle* software includes tools for simultaneously testing the astronomical forcing of paleoclimate data series and mean sedimentation rate with a correlation coefficient (COCO) approach, with an extension for testing the evolution of sedimentation rate (eCOCO) along the data series in the “Timeseries” menu (Li et al., 2018c). Similar methods for simultaneously testing for sedimentation rate and astronomical origins of stratigraphic data include the average spectral misfit (ASM) method of Meyers and Sageman (2007) (and its evolutionary extension eASM; Meyers, 2014), the Bayesian Monte Carlo method of Malinverno et al. (2010) and the TimeOpt method of Meyers (2015) (and its evolutionary extension eTimeOpt; Meyers, 2019). A comparison of COCO, ASM and TimeOpt is presented in Li et al. (2018c).

COCO estimates the correlation coefficient between power spectra of a sedimentary proxy series in the stratigraphic (depth) domain and an astronomical solution in the time domain, converting the proxy series from depth to time for a range of “test” sedimentation rates. The most likely sedimentation rate corresponds to the one resulting in the highest correlation coefficient. The COCO method is described in Li et al. (2018c), summarized as follows.

The Pearson product-moment correlation coefficient (Mudelsee, 2010; Pearson, 1895; Press et al., 1992) is used:

$$\rho(T, D) = \frac{1}{N-1} \sum_{i=1}^N \left(\frac{T_i - \mu_T}{\sigma_T} \right) \left(\frac{D_i - \mu_D}{\sigma_D} \right) \quad (5)$$

where N is the number of observations of the target (T) or data (D) time series, μ_T and σ_T are the mean and standard deviation of the target, and μ_D and σ_D are the mean and standard deviation of the data series. The correlation coefficient measures the linear correlation between the target (T) and data (D) series; in this case, the target series is the unsmoothed periodogram of the astronomical solution, and the data series

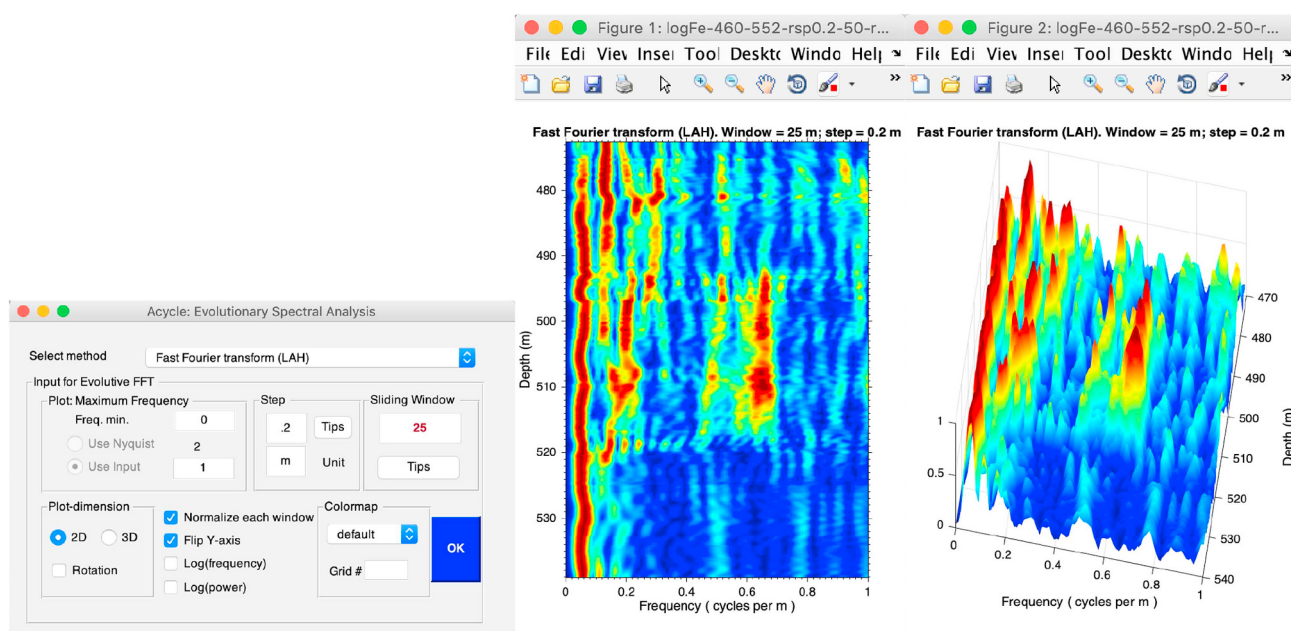


Fig. 7. Left panel: The “Evolutionary Power Spectral Analysis” GUI. Middle panel: evolutionary FFT spectrum of the log(Fe) series of Core BH9/05 after removing a 50 m “rLOESS” trend. Right panel: 3D evolutionary FFT spectrum of the log(Fe) series. Both middle and right panels use the same running window length of 25 m and a sliding step of 0.2 m.

is the unsmoothed periodogram of paleoclimate time series at a “test” sedimentation rate.

The assumption of no astronomical forcing (null hypothesis, H_0) is tested using a Monte Carlo simulation procedure that involves generating correlation coefficients between the power spectrum of the target and surrogate power spectra of the data constructed from random frequencies with random spectral amplitudes (Li et al., 2018c). The null hypothesis significance level indicates the probability that a specific correlation coefficient value can occur by chance. The null hypothesis significance level of 1% means that the original data-model correlation coefficient value exceeds 99% of the Monte Carlo simulated values. The number of astronomical parameters contributing to the correlation coefficient of each test sedimentation rate is also evaluated (Li et al., 2018c). If a low significance level of the null hypothesis is derived from the fact that only a few of the total number of astronomical parameters are used in the estimation, a high correlation coefficient value, in that case, may be suspicious. However, if a small sliding window is adopted, long orbital eccentricity cycles might not be detected, and the three precession index cycles may also be merged, generating valid COCO and eCOCO results even for a small number of contributing astronomical parameters.

The average sedimentation rate of the log(Fe) series of Core BH9/05 is evaluated using the COCO method. The COCO results show 2 peaks at 19.2 cm/kyr and 4.8 cm/kyr with the highest peak at 19.2 cm/kyr (Fig. 8). This indicates the mean sedimentation rate at Core BH9/05 is probably 19.2 cm/kyr. The null hypothesis significance level is no larger than 1% at 4.8 and 19.2 cm/kyr, indicating the null hypothesis of no astronomical forcing involved can be rejected at > 99% significance level. A sedimentation rate of 19.2 cm/kyr involves 5 astronomical parameters. This is acceptable because the total length of the dataset is too small to reveal significant 405 kyr long eccentricity cycles (e.g., power spectrum in Fig. 6). This sedimentation rate of 19.2 cm/kyr generally matches with the mean sedimentation rate of 21.5 cm/kyr reported by Charles et al. (2011). The wide range of the peak at 19.2 cm/kyr likely suggest the sedimentation rates may be variable throughout this series. Therefore, the eCOCO function that is designed to track variable sedimentation rates (Li et al., 2018c) is employed below.

For eCOCO analysis, the COCO procedure is extended to a sliding window along the data series. The sliding procedure, termed evolutionary correlation coefficient (eCOCO) highlights relatively stable sedimentation rates (Fig. 9) estimated along the log(Fe) series, revealing a best fit sedimentation rate of 16–19 cm/kyr in the 509–534 m PETM “body” interval, which slightly decreases to 13–14 cm/kyr in the PETM “recovery” interval (487–509 m). Subsequently, two options exist after the PETM event at 480 m: (1) sedimentation rates increase gradually to 21 cm/kyr; (2) sedimentation rates decrease to about 7 cm/kyr. Sedimentation rates in other continental margin sections increase multiple times within the PETM “body” interval (John et al., 2008) and drop after the PETM (Sluijs et al., 2008). Our result shows a higher resolution sedimentation rate map than that by Charles et al. (2011) for the BH9/05 core covering the PETM interval. Due to the lack of data and chronostratigraphic constraints for the pre-PETM and post-PETM intervals, the increased sedimentation rate during the PETM “body” interval must be tested elsewhere.

4.8. Filtering

Filters are essential tools to aid in the isolation of specific frequency components in paleoclimate data series. Low-pass filters are useful to isolate the low-frequency components (similar to the “smoothing” to tracking secular trend) of a data series, and high-pass filters are used to isolate the high-frequency components of a data series. Band-pass filtering is valuable for isolating specific frequency bands that may relate to Milankovitch forcing frequencies or other climate forcing frequencies. Frequency-domain filters are considered the most effective in cyclostratigraphy as they impose no time delay (thus “zero-phase”) in the filtered output: The data are Fourier transformed into the frequency domain, multiplied by the filter, then inverse-Fourier transformed back to the original domain (Kodama and Hinnov, 2015). Acycle includes a toolbox for filtering including Gauss and Taner algorithms (Taner, 2000) through *gaussfilter.m* and *tanerfilter.m*, (Kodama and Hinnov, 2015) (Fig. 10). The gain function defines how the amplitudes of the time series components change as a function of frequency during filtering design. The frequency and phase responses of both Gauss and Taner filters demonstrate that zero phase is maintained through the

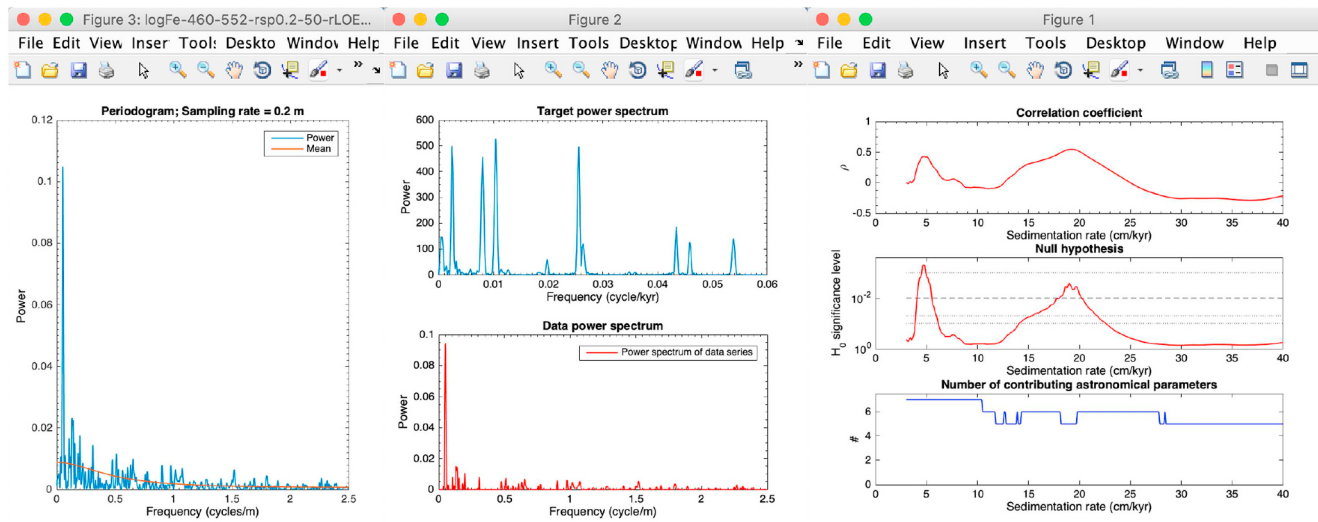


Fig. 8. COCO analysis of the detrended Fe series of Core BH9/05. Left panel: Unsmoothed periodogram of the entire log(Fe) series with the conventional AR(1) model. Middle panel: Unsmoothed periodogram of the astronomical solution (Laskar et al., 2004, 55–57 Ma; top) and the entire log(Fe) series after removing the AR (1) model (bottom). Right panel: The correlation coefficient results show potential sedimentation rates at 4.8 cm/kyr and 19.2 cm/kyr (top). Null hypothesis (H_0 , no astronomical forcing) testing of the data series indicates that 4.8 cm/kyr and 19.2 cm/kyr sedimentation rates have H_0 significance levels less than 1%. Significance levels are estimated using Monte Carlo simulation of 2000 iterations (middle). The number of contributing astronomical parameters in the tested sedimentation rates (bottom). Tested sedimentation rates range from 3 to 40 cm/kyr with a step of 0.1 cm/kyr.

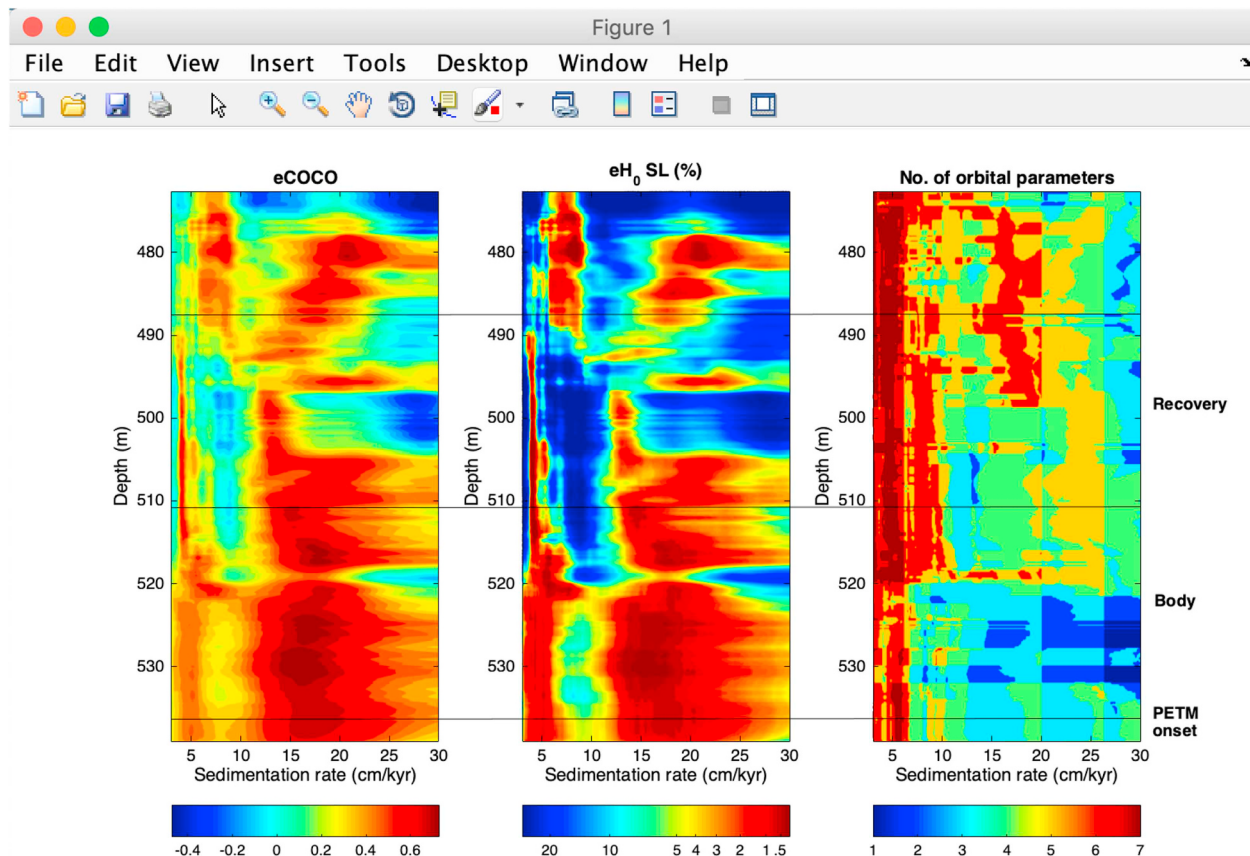


Fig. 9. eCOCO results of the Fe series from Core BH9/05. Left panel: Evolutionary correlation coefficient. Middle panel: Evolutionary H_0 significance level. Right panel: Evolutionary number of contributing astronomical parameters. The sliding window size is 25 m; the sliding window step is 0.2 m. All periodograms remove the conventional AR(1) red noise model. The number of Monte Carlo simulations is 2000. Sedimentation rates range from 3 to 30 cm/kyr with a step of 0.1 cm/kyr. (For interpretation of the references to color in this figure legend, the reader is referred to the Web version of this article.)

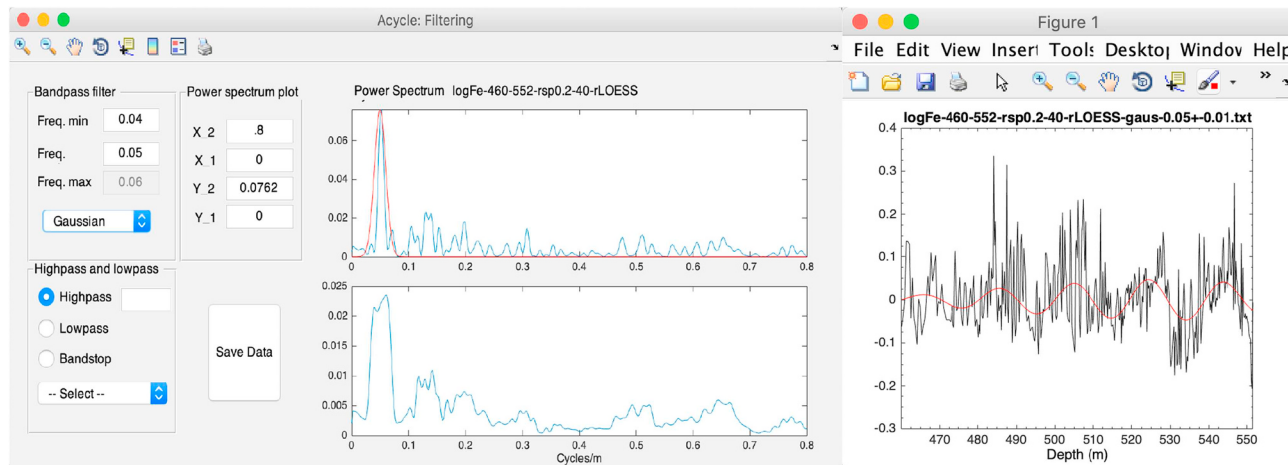


Fig. 10. (Left panel) Filtering toolbox. (Right panel) $\log(\text{Fe})$ series are shown with their Gauss bandpass-filtered outputs (passband: 0.05 ± 0.01 cycles/m).

passband (Kodama and Hinnov, 2015). More information about filtering can be found in Weedon (2003) and Kodama and Hinnov (2015). Taner filter settings for the optimal extraction of Milankovitch signals from tuned geological datasets are discussed by Zeeden et al. (2018).

4.9. Age model and tuning

The “Age Scale” toolbox in *Acycle* is useful to transform original data (usually in the depth domain) to tuned data (usually in the time domain) when an age model file is available. The age model may be based on radioisotopic dating, magnetic reversal age boundaries, time anchors from biostratigraphic correlation, an astronomical age model, or combinations of dating (Hilgen et al., 2015). For example, the potential sedimentation rate determined by objective statistical methods (e.g., eCOCO in Section 4.7), a filtered signal from the data series can be used to reconstruct an age model by assigning depth of each filtered series maximum (or minimum) to a time value using *Acycle*’s “Build Age Model” function. Careful evaluation must be made when tuning, especially when an astronomical age model is used, because astronomical tuning can improperly confine data cyclicity into Milankovitch periods and lead to circular reasoning (Kodama and Hinnov, 2015).

4.10. Sedimentary noise model

A sedimentary noise model was recently developed for the reconstruction of past sea-level changes from astronomically forced marginal marine stratigraphy (Li et al., 2018a). The model estimates sedimentary noise that is embedded in the data. The noise that affected climate and sea level includes: (i) water-depth-related noise such as storms, bioturbation, and unsteady sedimentation rate; (ii) proxy-related noise such as proxy sensitivity, measurement error, and dating error; and (iii) other factors including tectonics, diagenesis, and volcanism (Li et al., 2018a). Change in water-depth related noise at a fixed location in the marginal marine environment is taken as a proxy of relative sea-level. The sedimentary noise model for sea-level changes can also be applied to lacustrine basins because the evolution of terrestrial basins can also be linked to water level changes, and these changes can lead to variable sedimentary noise in paleoclimate proxies.

The sedimentary noise model includes two complementary approaches: lag-1 autocorrelation coefficient (ρ_1) and dynamic noise after orbital tuning (DYNOT). The definition of ρ_1 is given in Eq. (4). The advantage offered by ρ_1 is that it evaluates time series directly and is independent of frequency band selections. It can also work with series in stratigraphic domain. The DYNOT approach evaluates the ratio of non-orbital signal variance to the total variance, which is calculated along a sliding window in time domain. The variance ratios are

obtained from 2π multi-taper variance (power) spectra calculated along a sliding time window using the MatLab script *pda.m* (Li et al., 2016). The noise after removal of the orbital variance in a given time interval is given by Li et al. (2018a):

$$R = 1 - \frac{\sum P_{(e)} + \sum P_{(o)} + \sum P_{(p)}}{\sum_{i=f_{\min}}^{f_{\max}} P_{(i)}} \quad (6)$$

where f_{\min} and f_{\max} are cutoff frequencies for estimation of total variance between $f_{\min} = 0.001 \text{ kyr}^{-1}$, and $f_{\max} = 1 \text{ kyr}^{-1}$. $\sum P_{(e)}$, $\sum P_{(o)}$, and $\sum P_{(p)}$ are the power of orbital eccentricity, obliquity and precession index signals. When sea-level is relatively high, the DYNOT ratio is lower than the ratio in a time of relatively low sea-level, and vice versa. Increased noise leads to a decreased ρ_1 value, and vice versa.

Both approaches are included in *Acycle*. Details of these sedimentary noise models with case studies are provided in Li et al. (2018a).

5. Toolboxes, help menu and supporting documents

The software comes with a simple mathematical function (Eq. (7)), popular astronomical solutions, and demonstration paleoclimate data (Fig. 11). The simple mathematical function can generate a new data series based on the selected data. Both the first and second columns can be modified using given parameters:

$$X_i = a \times x_i + b, \quad (i = 1, 2, \dots, n) \quad (7)$$

where x_i is the i th member of either the first or the second column of selected data and X_i is the new data value from user defined parameters of a and b . n is the total number of rows of the selected dataset.

The popular astronomical solutions are the nominal astronomical solutions of eccentricity, obliquity, and precession including La2004 (Laskar et al., 2004) and La2010 (Laskar et al., 2011) solutions, and

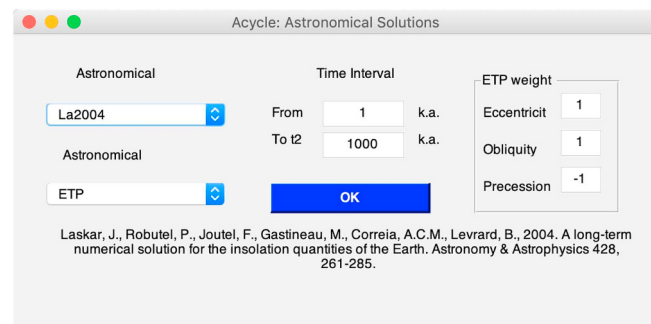


Fig. 11. Toolbox generating astronomical solutions.

orbital eccentricity and orbital inclination from astronomical solutions by Zeebe (2017). The 5-my long tuned stack of Pliocene-Pleistocene oxygen isotopes (Lisiecki and Raymo, 2005) is also included in *Acycle*. Users should cite the original publications if the astronomical solution or the oxygen isotope data are used in their project.

The Help menu provides information about the formats for the data files, and a variety of functionalities provided in the software. The revision history of the program, together with the contact address is included in the menu labeled “Read Me” and “Contact”. The software will be updated frequently, and the new version can be found in a menu labeled “Find Updates”. Sample time series and a User’s Guide with detailed instructions are provided to help the user understand and use the software.

6. Other software for paleoclimate time series analysis

There are several other popular software packages for paleoclimate series analysis and cyclostratigraphy: *Astrochron*, *AnalySeries*, *QAnalySeries*, *SSA-MTM* toolkit, *PAST*, *REDFIT*, *kSpectra*, *Arand*, and others. The open source software *Astrochron* (Meyers, 2014) has recently become one of the most popular and powerful programs in cyclostratigraphy. It uses the R language, and is maintained by Stephen R. Meyers at University of Wisconsin–Madison. *Astrochron* includes two separate statistical tests of astronomical forcing and estimation of sedimentation rates using the ASM (and eASM) and TimeOpt (and eTimeOpt) methods (see Section 3.6). *Astrochron* is available at <https://CRAN.R-project.org/package=astrochron>. For novice users, specific examples are provided in the *Astrochron* help documents. The *AnalySeries* 2.0.8 is a simple but powerful tool in cyclostratigraphy, but is limited to the Mac OS platform and has no help documentation (Paillard et al., 1996). *QAnalySeries* is new software written in Qt SDK that re-implements the major functionality of *AnalySeries* (Kotov and Pálike, 2018), and can be run on Mac OS, Windows and Linux systems (at <https://www.marum.de/en/Dr.-sergei-kotov/Software-2.html>). The *SSA-MTM* toolkit has been widely used in time series analysis due to its power in spectral analysis and signal-to-noise detection and is implemented on Unix (Linux) and Mac OS (Ghil, 1997) (at <http://research.atmos.ucla.edu/tcd//ssa/>). The *PAST* software is designed for paleontological data analysis with functions for univariate and multivariate statistics, ecological analysis, time series and spatial analysis, and stratigraphy (Hammer et al., 2001) (at <https://folk.uio.no/ohammer/past/>). *PAST* works with Windows and Mac OS. *REDFIT* is a Windows-based spectral analysis software package (Schulz and Mudelsee, 2002) that estimates red-noise spectra directly from irregularly spaced time series, without requiring interpolation. The *kSpectra* Toolkit from SpectraWorks (<http://www.spectraworks.com/>) is for Mac OS.

In comparison, *Acycle* runs on both Mac and Windows with MATLAB and is available as stand-alone software. With its graphic user interface, the *Acycle* software is easy to use and understand since no coding experience is needed. *Acycle* includes unique functions such as correlation coefficient analysis and sedimentary noise model for sea level, not included in the above packages. Furthermore, the *Acycle* software is also characterized by its educational purpose.

7. Summary

Acycle is a convenient and powerful program for performing analysis of depth- and time-series, providing advanced visualization, publication-quality graphics, and saving results. With its graphical user interface, the software is easy to use and understand. Our experience shows that this software facilitates the training of students in time series analysis, especially for studies in paleoclimatology and astrochronology as part of integrated stratigraphy.

Acycle reads and writes delimited data files with the ability to sort and select data slices. The integrated toolboxes conduct detrending with

multiple approaches to track and remove secular trends. Functions for power spectral analysis are available for the detection of periodic signals and the background spectrum. *Acycle* can generate pseudo-color and 3D plots of the evolutionary power spectrum to track variable frequencies. For astrochronology, a correlation coefficient function estimates optimal sedimentation rate and an evolutionary correlation coefficient function tracks variable sedimentation rates along sedimentary records. Finally, *Acycle* models sedimentary “noise” and provides options for hypothesis testing. Analytical results and graphical output can be printed and saved.

Notice: *Acycle* analyzes time series with user-defined parameters. The responsibility for the reliability of the data and correct interpretation lies with the user.

Authorship statement

Mingsong Li co-designed this study, designed the *Acycle* software, prepared all figures, and co-wrote the text. Linda Hinnov co-designed the study, contributed key scripts of the software, and co-wrote the text. Lee Kump contributed to the data interpretation and co-wrote the text.

Link to the code

The *Acycle* website is www.mingsongli.com/acycle, and the software can be downloaded from <https://github.com/mingsongli/acycle>.

Computer code availability

Acycle was developed by Mingsong Li with contributions from Linda Hinnov. Contact address of Mingsong Li is 410 Deike Bldg, University Park, PA 16802, USA. Tel: +1-(410)504-2885; e-mail: mul450@psu.edu, limingsonglms@gmail.com. Contact address of Linda Hinnov is 3457 Exploratory Hall, George Mason University, Fairfax, VA 22030, USA. Tel: +1-(703)993-8072; e-mail: lhinnov@gmu.edu. *Acycle* was first made available in 2018. There is no specific requirement for hardware. Operating systems include Windows XP or later and Mac OS X 10.6 or later. *Acycle* was developed using MATLAB version 2015b and 2017a. MATLAB is essential for the MATLAB version of the *Acycle* package. And MATLAB runtime (free, available at: www.mathlab.com) is required for the *Acycle* stand-alone software. The size of *Acycle* (MATLAB version) is 50 MB. The size of *Acycle* (stand-alone version) is 100 MB. The official website for *Acycle* is www.mingsongli.com/acycle, and the software can be downloaded from: <https://github.com/mingsongli/acycle>. A User’s Guide can be downloaded from https://github.com/mingsongli/acycle/blob/master/doc/AC_Users_Guide.pdf.

Research data

Acycle can be downloaded from <https://github.com/mingsongli/acycle>.

Conflicts of interest

The authors declare no competing interests.

Declarations of interest

None.

Acknowledgements

This project was funded by the Heising-Simons Foundation, United States (2016–11). This is a contribution to the IGCP Project 652. We thank Pauline Collon, Mathieu Martinez, and two anonymous reviewers for their constructive comments.

Appendix A. Supplementary data

Supplementary data to this article can be found online at <https://doi.org/10.1016/j.cageo.2019.02.011>.

References

- Box, G.E., Jenkins, G.M., 1976. *Time Series Analysis: Forecasting and Control*. Holden-day Revised Edition.
- Charles, A.J., Condon, D.J., Harding, I.C., Pälike, H., Marshall, J.E.A., Cui, Y., Kump, L., Croudace, I.W., 2011. Constraints on the numerical age of the Paleocene-Eocene boundary. *Geochem. Geophys. Geosyst.* 12. <https://doi.org/10.1029/2010GC003426>.
- Cui, Y., Kump, L.R., Ridgwell, A.J., Charles, A.J., Junium, C.K., Diefendorf, A.F., Freeman, K.H., Urban, N.M., Harding, I.C., 2011. Slow release of fossil carbon during the Palaeocene-Eocene Thermal Maximum. *Nat. Geosci.* 4, 481–485.
- Ghil, M., 1997. The SSA-MTM Toolkit: applications to analysis and prediction of time series. In: Optical Science, Engineering and Instrumentation, vol. 97. International Society for Optics and Photonics, pp. 216–230.
- Gilman, D., Fuglister, F., Mitchell Jr., J., 1963. On the power spectrum of “red noise”. *J. Atmos. Sci.* 20 (2), 182–184.
- Hammer, Ø., Harper, D., Ryan, P., 2001. PAST: paleontological statistics software package for education and data analysis. *Palaeontol. Electron.* 4, 1–9.
- Herbert, T.D., 1994. Reading orbital signals distorted by sedimentation: models and examples. In: de Boer, P.L., Smith, D.G. (Eds.), *Orbital Forcing and Cyclic Sequences*, vol. 19. pp. 483–507. <https://doi.org/10.1002/9781444304039.ch29>.
- Hilgen, F.J., Hinnov, L.A., Abdul Aziz, H., Abels, H.A., Batenburg, S., Bosmans, J.H.C., de Boer, B., Hüsing, S.K., Kuiper, K.F., Lourens, L.J., Rivera, T., Tuenter, E., Van de Wal, R.S.W., Wotzlaw, J.-F., Zeeeden, C., 2015. Stratigraphic continuity and fragmentary sedimentation: the success of cyclostratigraphy as part of integrated stratigraphy. Geological Society, London, Special Publications 404, 157–197.
- Hinnov, L.A., Wu, H., Fang, Q., 2016. Reply to the comment on “Geologic evidence for chaotic behavior of the planets and its constraints on the third-order eustatic sequences at the end of the Late Paleozoic Ice Age” by Qiang Fang, Huaijun Wu, Linda A. Hinnov, Xiuchun Jing, Xunlian Wang, and Qingchun Jiang [Palaeogeography Palaeoclimatology Palaeoecology 400 (2015) 848–859]. *Palaeogeogr. Palaeoclimatol. Palaeoecol.* 461, 475–480.
- Husson, D., 2014. MathWorks File Exchange: RedNoise_ConfidenceLevels. http://www.mathworks.com/matlabcentral/fileexchange/45539-rednoise-confidencelevels/content/RedNoise_ConfidenceLevels/RedConf.m.
- John, C.M., Bohaty, S.M., Zachos, J.C., Sluijs, A., Gibbs, S., Brinkhuis, H., Bralower, T.J., 2008. North American continental margin records of the Paleocene-Eocene thermal maximum: implications for global carbon and hydrological cycling. *Paleoceanography* 23. <https://doi.org/10.1029/2007PA001465>.
- Kodama, K.P., Hinnov, L., 2015. Rock Magnetic Cyclostratigraphy. Wiley-Blackwell.
- Kotov, S., Pälike, H., 2018. QAnalySeries – a Cross-Platform Time Series Tuning and Analysis Tool. AGU Fall Meeting, Washington DC.
- Laskar, J., Fienga, A., Gastineau, M., Manche, H., 2011. La2010: a new orbital solution for the long-term motion of the Earth. *Astron. Astrophys.* 532. <https://doi.org/10.1051/0004-6361/201116836>.
- Laskar, J., Robutel, P., Joutel, F., Gastineau, M., Correia, A.C.M., Levrard, B., 2004. A long-term numerical solution for the insolation quantities of the Earth. *Astron. Astrophys.* 428, 261–285.
- Li, M., Hinnov, L.A., Huang, C., Ogg, J.G., 2018a. Sedimentary noise and sea levels linked to land-ocean water exchange and obliquity forcing. *Nat. Commun.* <https://doi.org/10.1038/s41467-018-03454-y>.
- Li, M., Huang, C., Hinnov, L., Chen, W., Ogg, J., Tian, W., 2018b. Astrochronology of the Anisian stage (Middle Triassic) at the Guandao reference section, South China. *Earth Planet. Sci. Lett.* 482, 591–606.
- Li, M., Huang, C., Hinnov, L., Ogg, J., Chen, Z.-Q., Zhang, Y., 2016. Obliquity-forced climate during the Early Triassic hothouse in China. *Geology* 44, 623–626.
- Li, M., Kump, L.R., Hinnov, L.A., Mann, M.E., 2018c. Tracking variable sedimentation rates and astronomical forcing in Phanerozoic paleoclimate proxy series with evolutionary correlation coefficients and hypothesis testing. *Earth Planet. Sci. Lett.* 501, 165–179.
- Lisiecki, L.E., Raymo, M.E., 2005. A Pliocene-Pleistocene stack of 57 globally distributed benthic $\delta^{18}\text{O}$ records. *Paleoceanography* 20, PA1003. <https://doi.org/10.1029/2004PA001071>.
- Lomb, N.R., 1976. Least-squares frequency analysis of unequally spaced data. *Astrophys. Space Sci.* 39, 447–462.
- Malinverno, A., Erba, E., Herbert, T.D., 2010. Orbital tuning as an inverse problem: chronology of the early Aptian oceanic anoxic event 1a (Sellier Level) in the Cismone APICORE. *Paleoceanography* 25. <https://doi.org/10.1029/2009pa001769>.
- Mann, M.E., Lees, J.M., 1996. Robust estimation of background noise and signal detection in climatic time series. *Clim. Change* 33, 409–445.
- Martinez, M., 2018. Chapter Four - mechanisms of preservation of the eccentricity and longer-term Milankovitch cycles in detrital supply and carbonate production in hemipelagic marl-limestone alternations. In: Montenari, M. (Ed.), *Stratigraphy & Timescales*. Academic Press, pp. 189–218.
- Martinez, M., Kotov, S., De Vleeschouwer, D., Pas, D., Pälike, H., 2016. Testing the impact of stratigraphic uncertainty on spectral analyses of sedimentary series. *Clim. Past* 12, 1765–1783.
- Meyers, S.R., 2014. Astrochron: an R Package for Astrochronology. <http://cran.r-project.org/package=astrochron>.
- Meyers, S.R., 2015. The evaluation of eccentricity-related amplitude modulation and bundling in paleoclimate data: an inverse approach for astrochronologic testing and time scale optimization. *Paleoceanography*. <https://doi.org/10.1002/2015PA002850>.
- Meyers, S.R., 2019. Cyclostratigraphy and the problem of astrochronologic testing. *Earth Sci. Rev.* 190, 190–223.
- Meyers, S.R., Hinnov, L.A., 2010. Northern Hemisphere glaciation and the evolution of Plio-Pleistocene climate noise. *Paleoceanography* 25, PA3207. <https://doi.org/10.1029/2009pa001834>.
- Meyers, S.R., Sageman, B.B., 2007. Quantification of deep-time orbital forcing by average spectral misfit. *Am. J. Sci.* 307, 773–792.
- Meyers, S.R., Sageman, B.B., Arthur, M.A., 2012. Obliquity forcing of organic matter accumulation during Oceanic Anoxic Event 2. *Paleoceanography* 27. <https://doi.org/10.1029/2012pa002286>.
- Mudelsee, M., 2002. TAUEST: a computer program for estimating persistence in unevenly spaced weather/climate time series. *Comput. Geosci.* 28, 69–72.
- Mudelsee, M., 2010. Climate Time Series Analysis. Springer International Publishing, pp. 454.
- Paillard, D., Labeyrie, L., Yiou, P., 1996. Macintosh program performs time-series analysis. *Eos, Transactions American Geophysical Union* 77 379–379.
- Pearson, K., 1895. Mathematical contributions to the theory of evolution—III. Regression, heredity, and panmixia. *Philos. Trans. R. Soc. London, Ser. A* 187, 253–318.
- Press, W.H., Teukolsky, S.A., Vetterling, W.T., Flannery, B.P., 1992. Numerical Recipes in C. Cambridge University Press, Cambridge, pp. 925.
- Prokopenko, A.A., Hinnov, L.A., Williams, D.F., Kuzmin, M.I., 2006. Orbital forcing of continental climate during the Pleistocene: a complete astronomically tuned climatic record from Lake Baikal, SE Siberia. *Quat. Sci. Rev.* 25, 3431–3457.
- Rodionov, S.N., 2006. Use of prewhitening in climate regime shift detection. *Geophys. Res. Lett.* 33. <https://doi.org/10.1029/2006GL025904>.
- Scargle, J.D., 1982. Studies in astronomical time series analysis. II-Statistical aspects of spectral analysis of unevenly spaced data. *Astrophys. J.* 263, 835–853.
- Schulz, M., Mudelsee, M., 2002. REDFIT: estimating red-noise spectra directly from unevenly spaced paleoclimatic time series. *Comput. Geosci.* 28, 421–426.
- Schulz, M., Stattegger, K., 1997. SPECTRUM: spectral analysis of unevenly spaced paleoclimatic time series. *Comput. Geosci.* 23, 929–945.
- Sluijs, A., Röhl, U., Schouten, S., Brumsack, H.-J., Sangiorgi, F., Sinninghe Damsté, J.S., Brinkhuis, H., 2008. Arctic late Paleocene–early Eocene paleoenvironments with special emphasis on the Paleocene-Eocene thermal maximum (Lomonosov Ridge, Integrated Ocean Drilling Program Expedition 302). *Paleoceanography* 23. <https://doi.org/10.1029/2007PA001495>.
- Tanner, M.T., 2000. Attributes Revisited. Technical Publication, Rock Solid Images, Inc., Houston, Texas. <https://www.rocksolidimages.com/attributes-revisited/>, Accessed date: 7 January 2019.
- Thomson, D.J., 1982. Spectrum estimation and harmonic analysis. *Proc. IEEE* 70, 1055–1096.
- Thomson, D.J., 2009. Time-Series Analysis of Paleoclimate Data, Encyclopedia of Paleoclimatology and Ancient Environments. Springer, pp. 949–959.
- Weedon, G.P., 2003. Time Series Analysis and Cyclostratigraphy: Examining Stratigraphic Records of Environmental Cycles. Cambridge University Press, pp. 259.
- Zeebe, R.E., 2017. Numerical solutions for the orbital motion of the solar system over the past 100 Myr: limits and new results. *Astron. J.* 154, 193. <https://doi.org/10.3847/1538-3881/aa8cce>.
- Zeeeden, C., Kaboth, S., Hilgen, F.J., Laskar, J., 2018. Taner filter settings and automatic correlation optimisation for cyclostratigraphic studies. *Comput. Geosci.* 119, 18–28.